MCADAM: A continuous paleomagnetic dipole moment model for at least 3.7 billion years

Richard K. Bono[1], Greig A. Paterson[2], and Andrew J. Biggin[2]

[1]Department of Earth, Ocean and Atmospheric Science, Florida State University, FL 32304, USA
[2]Department of Earth, Ocean and Ecological Sciences, University of Liverpool, Liverpool L697ZE, UK

Key Points:

- Continuous dipole moment models for the past 3.7-4.2 billion years are presented
- Our model reproduces salient features of the paleomagnetic dipole field
- Paleomagnetosphere estimates suggest Precambrian atmospheric shielding was much weaker than present day
- Est. length: 3900 words (8 PU), 4 figures (4 PU)

Corresponding author: Richard K. Bono, `rbono@fsu.edu`

Abstract

Understanding the evolution of Earth's magnetic field can provide insights into core processes and can constrain plate tectonics and atmospheric shielding. The PINT absolute paleointensity database provides a curated repository of site mean, i.e., cooling unit, estimates of the strength of the magnetic field. We present a minor update to the PINT database to version 8.1 by adding 199 records from 25 studies published primarily from 2019 through 2022. The PINT database is used to define a continuous model of the dipole field, using an approach combining non-parametric and Monte Carlo resampling termed MCADAM. Three dipole field strength models spanning 50 ka to 3.7-4.2 Ga (MCADAM.1a-c) are presented, reflecting three tiers of increasingly more stringent data selection thresholds. The MCADAM dipole field models allow for the estimation of the magnetic standoff distance, constraining the shielding of Earth's atmosphere against solar wind erosion provided by the geodynamo.

1 Introduction

The evolution of Earth's deep interior since core formation (Nimmo, 2015) $>$ 4 billion years ago (Ga) remains a topic of considerable study. Obtaining information of the deep interior is generally restricted to present-day observations (e.g., seismic tomography). Alternatively, insights on processes occurring before the modern era require sampling geologic materials which formed at, or were transported to, Earth's surface. However, the geomagnetic field is generated in the liquid fraction of Earth's core through the geodynamo, and changes in the morphology, strength and variability in the geodynamo may reflect the evolution of core processes and the pattern of heat flux at the core-mantle boundary (CMB). The geomagnetic field is also a critical component for Earth's habitability (Rodríguez-Mozos & Moya, 2017) due to the protective envelope provided by the magnetosphere against atmospheric erosion by charged solar particles. It is speculated that changes in the paleomagnetosphere may have contributed to substantial changes in the evolution of life (e.g., Meert et al., 2016).

Paleomagnetic studies offer the potential to help close this gap: when rocks bearing magnetic carriers form the geomagnetic field imparts a remanence magnetization that, with ideal conditions and carriers, can be robustly preserved on the order of billions of years. The strength of the geodynamo can be described by the magnitude of the dipole moment, the first-degree spherical harmonic component of the field, which should reflect a long-term (time-averaged) trend and describes $\sim 90\%$ of the recent geomagnetic field. A fundamental question regarding Earth's dynamo is how the dipole moment has changed over long timescales ($\gg$ millions of years). Individual paleomagnetic specimens can be measured in the laboratory to quantify the strength of the remanent magnetization, or paleointensity, imparted into the specimen. Paleointensities measured from the same geologic time (e.g., from the same cooling-unit, referred to as a "site") can be related to paleointensities from other locations by transforming the paleointensity (B) into a virtual (axial) dipole moment (V(A)DM) using the following equation (Merrill et al., 1996)

$$VDM = \frac{4\pi {r_E}^3}{2\mu_0} B(1 + 3\cos^2 I)^{0.5} \tag{1}$$

where r_E is Earth's radius, μ_0 is vacuum permeability, and I is the inclination of the site derived from paleomagnetic directional measurements (there is an equivalent transformation to VADM using site paleolatitude). Virtual dipole moment transformations assert that the mean paleointensity measured at the site level can be entirely described by the dipole field, this simplification allows for comparisons from globally distributed observations on the strength of the field.

Characterizing the time-varying paleomagnetic field can be approached using several different methods. On geologically recent timescales ($<$ 100 thousand years, kyr), spherical harmonic models describe the morphology and strength of the field (e.g., Panovska et al., 2018). For the past 2 Myr, a continuous axial dipole moment model (Ziegler et al., 2011) can be constructed using relative paleointensity data from stacked sedimentary records combined with absolute paleointensity estimates, generally from volcanic sources. For longer timescales ($\gg$ 2 million years), dipole moment descriptions are substantially less well resolved. Tauxe and Staudigel (2004) reported a mean value for the 0-300 Ma interval, whereas Ingham et al. (2014) and Kulakov et al. (2019) applied a more complex reversible-jump Markov Chain Monte Carlo approach to define Mesozoic trends. Other approaches recently applied to the Precambrian field include binned data (e.g., Biggin et al., 2015), a low-degree polynomial fit (e.g., Bono et al., 2019), or sliding window average (e.g., Tarduno et al., 2020). These meta-analyses have proven important in providing observational constraints on dynamo and core evolution models (e.g., Biggin et al., 2015; Driscoll, 2016; Bono et al., 2019) and time-averaged and time-varying field estimates (e.g., Selkin & Tauxe, 2000; Ziegler et al., 2011).

The PINT database (`http://www.pintdb.org/;` Biggin et al., 2009; Bono et al., 2022) is a curated repository of absolute paleointensity records derived from volcanic sources and reported at the site mean level with associated meta-data, which makes it well-suited for paleointensity meta-analyses. In this study, we provide an incremental update to the PINT database (v8.1) that we use as the basis for a dipole moment evolution model (Section 2). In Section 3, we introduce a modeling framework, MCADAM (Monte Carlo Axial Dipole Average Model), that uses a combination of non-parametric site resampling, Monte Carlo simulations, and time-adaptive locally-weighted smoothing to produce a posterior distribution of field strength estimates from which a median dipole strength and associated predictive interval can be determined. Using the MCADAM framework and ***three*** filtered datasets from the PINT database that apply increasingly more stringent selection criteria, we present a suite of dipole moment evolution models that yield continuous predictions of the time-average (paleomagnetic) dipole moment extending back to the oldest paleomagnetic records from > 4 Ga, and compare these models with other time-average descriptions of field strength in deep time (Section 4) and the associated impact on the paleomagnetosphere (Section 5).

2 Updates to PINT v8.1

The PINT database underwent a significant update to version 8.0, and we refer readers to Bono et al. (2022) who describe the current structure of the database and broadly summarizes the distribution and quality of the paleointensity dataset. The most salient changes in PINT v8.0 with respect to prior versions of the PINT database (Biggin et al., 2015) are the inclusion of new paleointensity data published through the end of 2019, the removal of demonstrably biased paleointensity records (so-called "auto-zeros"), and the integration of Q_{PI} assessments for over 90% of the database. Q_{PI} (Quality of Paleointensity; Biggin & Paterson, 2014) is a semi-quantitative framework to describe the reliability of a site mean paleointensity record, and we again refer readers to Bono et al. (2022) for a complete description of Q_{PI} implementation in PINT v8.0.

In this study, we include a minor version update of PINT to v8.1 (1 that includes paleointensity records published in 2020 through July 2022. Included studies are not exhaustive of entire paleointensity dataset published during this interval, however, it represents a good-faith effort to identify as many relevant studies as possible. In total, ***230*** new sites from ***29*** studies have been added to the PINT v8.1 database. These data include contributions constraining the field during the Cambrian/Ediacaran (e.g., Thallner, Biggin, & Halls, 2021; Thallner, Biggin, McCausland, & Fu, 2021) and Neoproterozoic (e.g., Lloyd et al., 2021), which remain under-sampled relative to other geologic intervals.

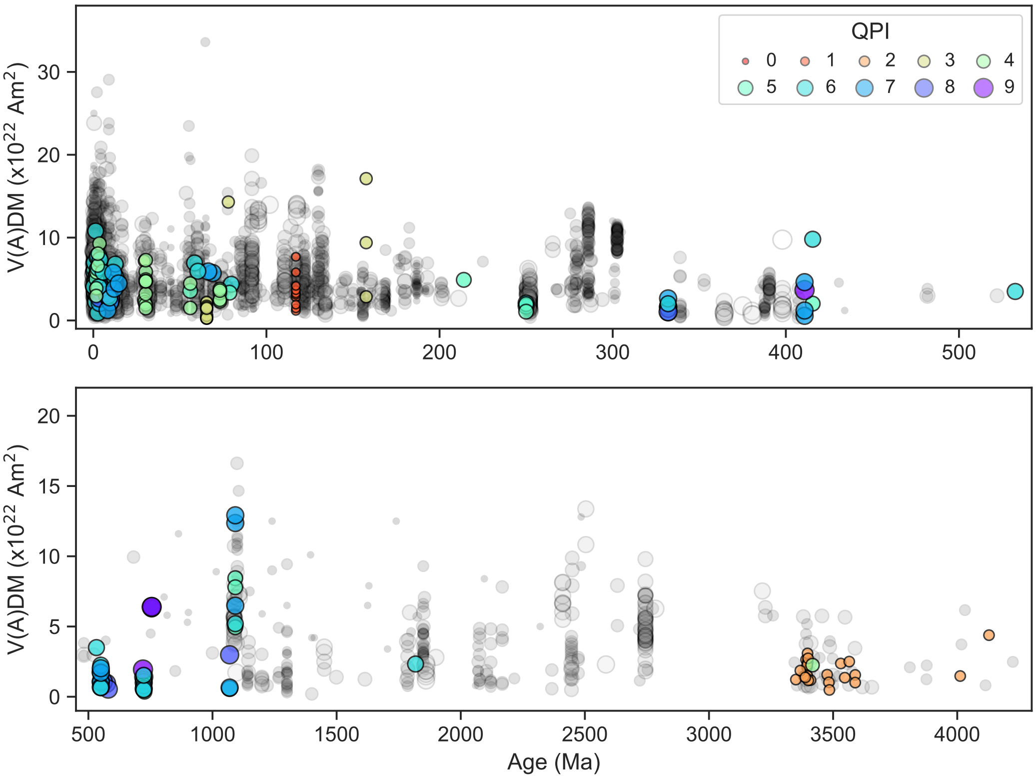

Figure 1. PINT v8.1 absolute paleointensity database. Colored circles show site mean records added since v8.0 (Bono et al., 2022); grey circles are data in PINT v8.0. Symbol size and color shows Q_{PI} score. Top: Phanerozoic; bottom: Precambrian.

The Q_{PI} criteria (Biggin & Paterson, 2014) serve two main purposes: first to act as a framework in the design and implementation of paleointensity research. Each individual criterion represents a pillar of best practice in paleointensity experimental design. While satisfying any or all the individual criterion does not guarantee that a given site mean paleointensity result reflects the true field strength, our confidence in the data should improve with increasing Q_{PI} criteria achievement (i.e., the data take into account key factors that are known to detrimentally impact the fidelity of the paleointensity recording). A second purpose of the Q_{PI} criteria is to facilitate the meta-analysis of the PINT database and site mean paleointensity-data. In particular, to enable more nuanced analysis outside of the paleomagnetic community, where the familiarity and historical context of how paleointensity data are collected and reported is less understood. Q_{PI} criteria allow for a semi-quantitative, objective definition of requirements to filter data from the PINT database, with the goal of improving the robustness of meta-analyses.

Field strength estimates are inherently challenging to extract from the rock record. Paleointensity specimens may be compromised by the presence of non-ideal magnetic recorders (e.g., multidomain grains) and/or laboratory alteration. The potential for remanences to be reset by thermal or chemical over-printing after emplacement must also be excluded before accepting a measured paleointensity as valid and meaningfully linked to the emplacement age. Several efforts have been made to identify useful heuristics and minimum analytical requirements to separate robust individual paleointensity results from suspect ones (e.g., Selkin & Tauxe, 2000; Kissel & Laj, 2004; Biggin et al., 2007). However, there is no clear consensus on what should be the minimum acceptable thresholds for paleointensity data at the specimen level, and propagating those decisions through to the site mean level often requires substantial discipline expertise and specific geologic context for the locality. Thus, applying a consistent data treatment in meta-analyses is often not feasible. While the Q_{PI} criteria do not reflect all aspects of paleointensity data (see Smirnov et al. (2016)), by providing individual Q_{PI} criteria and descriptive notes explaining the scoring process, the framework allows for informed decision making in the data selection process.

Since the data may reflect some non-ideal paleointensity biases, some fraction of the site mean data should be excluded from analyses in order to improve the robustness of any resulting conclusions drawn from using the PINT database. However, paleointensity data are sparse and imperfect individual records may still yield meaningful inferences in aggregate. Thus it is crucial to define selection criteria that balance data quality with data availability, specifically for the development of time-averaged and time-evolution field descriptions on million-to-billion-year timescales. Meta-analyses considering other topics will, of course, result in different optimal selection criteria choice.

Three different selection criteria are employed as examples for how the PINT database can be interrogated for meta-analysis, which have been previously presented in Bono et al. (2022). The first two filters are as follows: all data, and site mean $Q_{PI} \geq 3$. The third filter (introduced by Kulakov et al., 2019) prioritizes certain criteria and requires that site mean data meet the QAGE, QALT, and QMD criteria, thus requiring evidence that the site age is well constrained and the primary remanence is associated with the age estimate (QAGE) and there were experimental controls to limit the influence of laboratory alteration (QALT) and non-ideal (i.e., multidomain) magnetic carriers (QMD). We note that Smirnov et al. (2016) and Bono et al. (2019) previously identified PINT data which potentially under (over) estimate field strength fitting the shallow (steep) components of two-slope or concave Arai diagrams. Since this level of analysis was not applied to all records within PINT v8.1, we have not excluded the identified sites *a priori*, however, we distinguish sites which may be biased in Figure 2b and all but two sites are excluded using our "strict" prioritized Q_{PI}selection criteria. In addition to the above selection criteria, sites explicitly described as having a transitional polarity were excluded.

3 Time-varying paleofield models with uncertainties

Here, we consider whether a continuous time-varying field model can be realized for the entire paleointensity record. Ideally, a time-varying dipole field strength model should take several factors into consideration. We chose to focus on the following requirements:

1. Data selection should balance quality with availability of data.
2. The model should not be overly sensitive to any given data point due to the sparse and non-uniform distribution of paleointensity site means in the PINT database.
3. The model should reflect the uncertainty of individual site mean estimates in both age and field strength.
4. The model should seek to average secular variation, taking into account the increasing sparsity of data going further back into geologic time.

To meet these requirements, we employ a combination of techniques, which we refer to as a Monte Carlo Axial Dipole Average Model (MCADAM). A complete description of the modelling approach is provided in Supplementary Text S1. In summary, a resampling algorithm using non-parametric resampling of site mean records combined with Monte Carlo realizations derived from site mean intensity, inclination and age (and associated uncertainties). An individual set of realizations are time-averaged using a LOWESS (local regression) approach (Cleveland, 1979), applying an adaptive kernel defined used a minimum number of sites (5) and reasonable age bounds (spanning 250 kyr to ~ 76

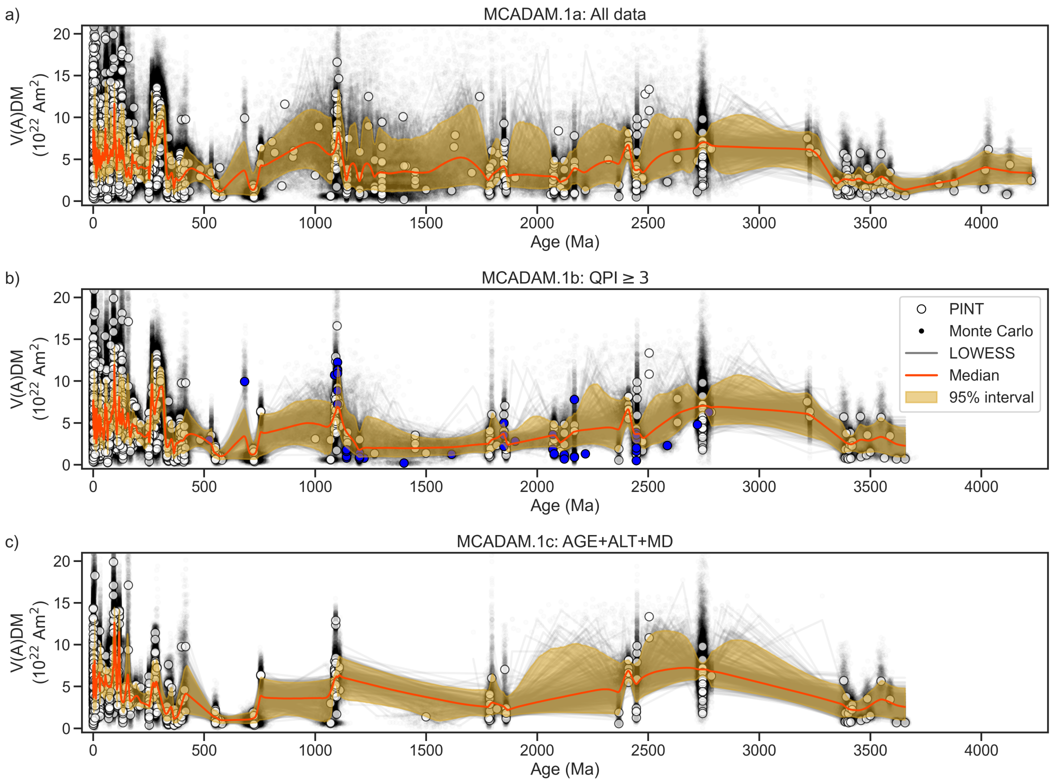

Figure 2. MCADAM time-varying model of paleofield strength for the past 3.7 to 4.2 billion years from PINT data. White circles: selected PINT data; black points, Monte Carlo realizations of PINT data; grey lines, individual MCADAM realizations; orange line, median time-varying model from MCADAM with shaded 95% interval. A) MCADAM.1a, all data in PINT v8.1; B) MCADAM.1b, Q_{PI} ≥3, blue circles mark sites which may be biased as identified by Smirnov et al. (2016) or Bono et al. (2019); C) MCADAM.1c, prioritized Q_{PI}: QAGE, QALT and QMD must be equal to 1.

Myr). The MCADAM modeling framework was tested using a synthetic data set with a known "true" dipole moment and a temporal distribution derived from PINT v8.1 (Supplementary Fig. S1).

4 Comparing MCADAM to other compilations

Applying the MCADAM approach with the PINT v8.1 dataset restricted by the three selection filters previously discussed (all data, Q_{PI}≥ 3, and prioritized selection QAGE+QALT+QMD), the resulting time-varying models (MCADAM.1a-c) are presented in Figure 2. Our preferred model is MCADAM.1b, which uses the a moderately restrictive dataset requiring that paleointensity site records meet at least three of the Q_{PI} criteria. In general, this model reproduces several characteristic features previously observed in the paleofield (Figure 3 and Supplementary Figures S2-S3), such as rise in field strength from the Matuyama to Brunhes chrons, intervals of high field strength during the Cretaceous Normal Superchron preceded by a weaker field (cf. the binned PINT analysis of Kulakov et al. (2019)), and a high field during the Kiaman Superchron (e.g., Cottrell et al., 2008) preceded by sustained weak field during the Devonian (Hawkins et al., 2019). For the 50 kyr to 2 Ma interval, there is good agreement between our model and that of PADM2M (Ziegler et al., 2011). Given the denser temporal sampling during the Phanerozoic, more variation in the field can be resolved with a smaller confidence interval for the resulting model relative to the Precambrian.

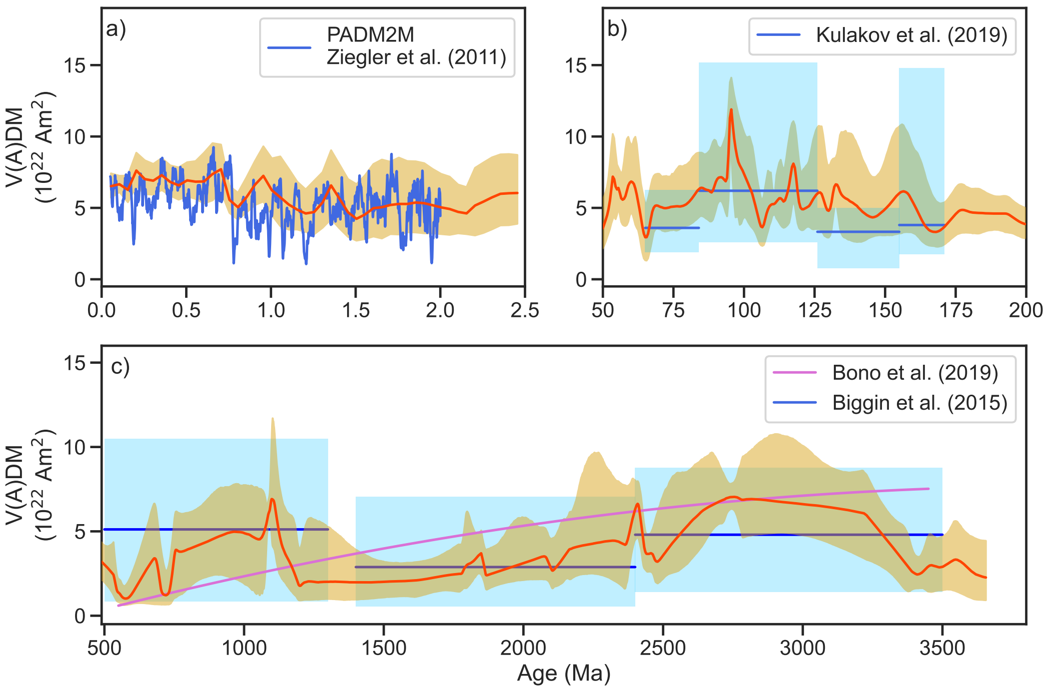

Figure 3. MCADAM.1b time-varying model of paleofield strength for the past 3.7 billion years from PINT v8.1 data meeting $Q_{PI} \geq$ 3 criteria. In all panels, the orange line represents the median time-varying model from MCADAM.1b with shaded 95% interval. A) Quaternary; blue line shows PADM2M model (Ziegler et al., 2011); b) Mesozoic; blue line and field shows median and 95% interval of Q_{PI} binned following (Kulakov et al., 2019); C) Precambrian; purple line shows polynomial fit of Bono et al. (2019), blue lines show bin medians with shaded 95% confidence intervals of Biggin et al. (2015).

The Paleozoic through the Precambrian poses the greatest challenge for characterizing the time-varying field due to large gaps in the PINT database. In our model, we use a linear interpolation between sampling, however given that intervals spanning ∼100 Myr may not sample the field at all, it is almost certain there are field variations that are not captured in our model. Given the combination of non-parametric resampling for data selection and using a Monte Carlo sampler based the selected data in the realization, we feel that the MCADAMmodels represent an overly smoothed description of the time varying field, particularly where the data are are sparse. We note that the oldest field records of the Archean are dominated by the Thellier-Coe zircon experiments of Tarduno et al. (2015, 2020), which due to their lack of orientation, represent a source of uncertainty in our model during the Eoarchean/Hadean. The fall and rise in field strength during the Mid- to Late- Proterozoic (as suggested by Biggin et al. (2015)) is supported by our model, as well as the drop in field strength at the end of the Proterozoic reported in Bono et al. (2019).

There are some general differences in the analyses of Biggin et al. (2015), Bono et al. (2019) and our study that can explain the apparent disagreement in estimated field trends. First, there are differences in the data sets used between both analyses, as summarized by Bono et al. (2019). Second, Biggin et al. (2015) divided the data sets into Early, Mid and Late Proterozoic bins and summarized the statistical properties of PINT records within each bin. Bono et al. (2019) focused *a priori* on estimates from slow-cooling intrusives (or select sites demonstrating time-averaged statistics) resulting in a substantially reduced data set compared to either this study or that of Biggin et al. (2015), and from this restricted data set estimated a 2^{nd} degree polynomial fit. In this study, we forgo both dividing the data into prescribed bins or focusing *a priori* on intrinsically time-averaged records. Our study uses a broader dataset, supplemented by new data published since the prior studies, that result in more variation in the interpreted dipole field strength relative to prior work.

5 Implications for the paleomagnetosphere

The geodynamo and the associated magnetic field extending into space provides shielding of Earth's atmosphere and surface water from erosion due to solar wind (Tarduno et al., 2014). In addition to increasing erosion of the atmosphere, reductions in magnetic shielding can drive breakdown of atmospheric ozone, which limits penetration of UVB radiation (Glassmeier & Vogt, 2010). Because of the protective ability of magnetospheres, a long-lived, robust magnetic field has been identified as one of the prerequisites for a habitable planet (Rodríguez-Mozos & Moya, 2017). Therefore, the strength and evolution of the magnetosphere is of critical interest. Currently, modelling the magnetosphere (or paleomagnetosphere) in detail requires fully coupled dynamo and solar activity simulations beyond the scope of what is available. However, a first-order approximation can be estimated using a series of reasonable simplifications, chiefly that the field is dipole-dominated (supported by Biggin et al., 2020) and that magnetic shielding can be approximated by the magnetic standoff distance, or magnetopause, where solar wind pressure is balanced by the repelling force of a dipole field (Siscoe & Sibeck, 1980). The present-day magnetopause is $\sim 10\ R_E$ (Earth radii) and will fluctuate on annual timescales as the magnetic pole moves about the spin axis (Shue et al., 1997).

Following the approach of Tarduno et al. (2010), the magnetic standoff distance, $r_s(t)$ for a given time t, can be estimated as the balance point between solar wind pressure and the dipole magnetic field (described by Siscoe & Chen, 1975),

$$r_s(t) = \left[\frac{\mu_0^2 f_0^2 M_E(t)^2}{4\pi^2(2\mu_0 P_{SW}(t) + B_{IMF}^2)}\right] \tag{2}$$

where μ_0 is vacuum permeability, f_0 is a field shape parameter for the magnetosphere (1.16 for present day Earth, Voigt (1995), held constant here), and B_{IMF} is the interplanetary field (which is neglected in our calculations since it is small, $\ll 10$ nT). M_E is the (paleo)magnetic dipole moment as a function of time. P_{SW} is the solar wind ram pressure, which is dependent on the mass loss rate of the sun and velocity of solar wind as a function of time. Extrapolating present day P_{SW} ($\sim$1.9 nPa, Shue et al. (1997)) back through time can be done with power-law model $(t/t_0)^{-2.33}$ based on solar analogs (e.g., Wood et al., 2005), at least until the young Hadean sun.

Using the MCADAM.1b model, the magnetic standoff distance from 50 ka to 3.7 Ga can be estimated (Figure 4 and Supplementary Figures S4-S5). The magnetopause responds rapidly to changes in either solar wind activity or the geomagnetic field and will vary by 1-2 R_E during typical space weather (Voigt, 1995). Coronal mass ejections and solar flares can suppress the standoff distance by half (e.g., the Halloween 2003 event was observed to reduce the magnetopause to $\sim 5\ R_E$, Rosenqvist et al. (2005)). While short term reductions ($\ll$ millions of years) in magnetic shielding are unlikely to impact the biosphere significantly, protracted intervals of reduced shielding may have affected

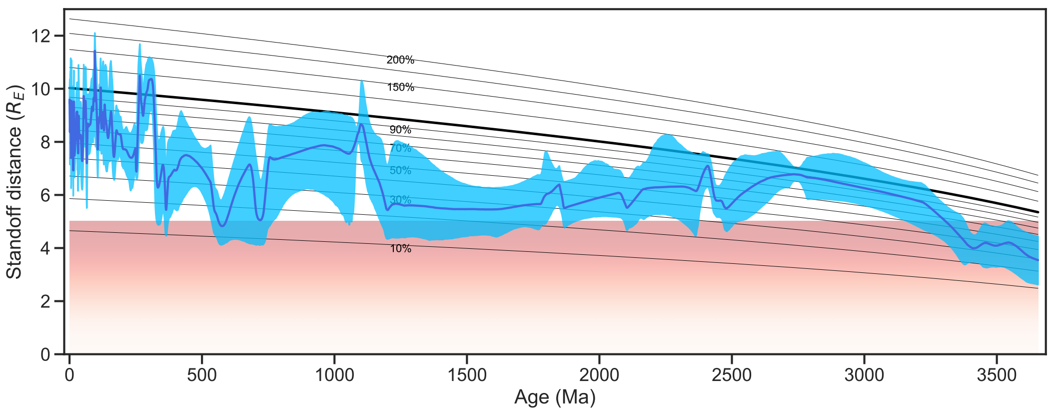

Figure 4. Magnetopause standoff distance estimate using equation 2 and the MCADAM.1b modeled dipole moment curve with PINT v8.1 data meeting $Q_{PI} \geq$ 3 criteria. Blue curve is the predicted median dipole moment and blue field is the 95% predicted interval. Contour lines show standoff distance relative to the present day. Red gradient shows standoff distance associated with the Halloween 2003 solar storm (Rosenqvist et al., 2005).

evolutionary processes (e.g., Meert et al., 2016; van der Boon et al., 2022). Our analysis suggests that the combination of the generally weaker Precambrian field and the increased solar wind associated with a younger, more active sun resulted in a long-term average standoff of ~ 5 R_E, which is about half the present-day magnetopause and consistent with the single zircon crystal estimates of Tarduno et al. (2010) for the early Archean. Individual snapshots or time-average estimates (on million-year or shorter timescales) suggest there were intervals with even further reduced standoff distances, e.g., the Ediacaran. These values represent a baseline standoff distance, which could be further reduced due to internal changes in the field (reduction or loss of dipolarity) or increases in solar wind activity (coronal mass ejections, solar flares). This implies that during the Proterozoic and Archean, atmospheric shielding by the magnetic field was potentially tenuous despite the robust, albeit weaker than present day, dipole field.

6 Conclusions

Using an updated PINT database, we have developed a new continuous dipole field modelling approach (MCADAM). Based on three approaches of selection data using Q_{PI} criteria, our MCADAM models can robustly recover the average dipole field strength and captures key features previously identified in the Quaternary (Ziegler et al., 2011), the

Mesozoic (Kulakov et al., 2019), and the Precambrian (Biggin et al., 2015; Bono et al., 2019).

We estimate the magnetic standoff distance from our preferred model MCADAM.1b and show that the after the earliest Archean, the standoff distance was less than half the present day distance of ~ 10 Earth radii due to the strong solar wind pressure streaming off the younger Sun. Following the Young Sun lows, the paleomagnetosphere experienced a protracted ($\sim 20-100$ Myr) minima during the Ediacaran, followed by a highly variable but generally increasing standoff distance in the Phanerozoic.

Acknowledgments

The authors acknowledge support from The Leverhulme Trust and NERC. R.K.B. acknowledges support for The Leverhulme Trust Early Career Fellowship (ECF-2020-617). G.A.P. is funded by a Natural Environment Research Council Independent Research Fellowship (NE/P017266/1). PINT v8.1 is provided as a Supplementary Data S1 and is also available at `http://www.pintdb.org/`. MCADAM.1a-c model outputs are available on the Earth Ref Data Archive, ERDA, at `http://www.earthref.org/ERDA/`.

References

Biggin, A. J., Bono, R. K., Meduri, D. G., Sprain, C. J., Davies, C. J., Holme, R., & Doubrovine, P. V. (2020). Quantitative estimates of average geomagnetic axial dipole dominance in deep geological time. *Nature Communications*, *11*(1), 6100. doi: 10.1038/s41467-020-19794-7

Biggin, A. J., & Paterson, G. A. (2014). A new set of qualitative reliability criteria to aid inferences on palaeomagnetic dipole moment variations through geological time. *Frontiers in Earth Science*, *2*. doi: 10.3389/feart.2014.00024

Biggin, A. J., Perrin, M., & Dekkers, M. J. (2007). A reliable absolute palaeointensity determination obtained from a non-ideal recorder. *Earth and Planetary Science Letters*, *257*(3), 545–563. doi: 10.1016/j.epsl.2007.03.017

Biggin, A. J., Piispa, E. J., Pesonen, L. J., Holme, R., Paterson, G. A., Veikkolainen, T., & Tauxe, L. (2015). Palaeomagnetic field intensity variations suggest Mesoproterozoic inner-core nucleation. *Nature*, *526*(7572), 245–248. doi: 10.1038/nature15523

Biggin, A. J., Strik, G. H. M. A., & Langereis, C. G. (2009). The intensity of the geomagnetic field in the late-Archaean: New measurements and an analysis of the updated IAGA palaeointensity database. *Earth, Planets and Space*, *61*(1), 9–22. doi: 10.1186/BF03352881

Bono, R. K., Paterson, G. A., van der Boon, A., Engbers, Y. A., Michael Grappone, J., Handford, B., . . . Biggin, A. J. (2022). The PINT database: A definitive compilation of absolute palaeomagnetic intensity determinations since 4 billion years ago. *Geophysical Journal International*, *229*(1), 522–545. doi: 10.1093/gji/ggab490

Bono, R. K., Tarduno, J. A., Nimmo, F., & Cottrell, R. D. (2019). Young inner core inferred from Ediacaran ultra-low geomagnetic field intensity. *Nature Geoscience*, *12*(2), 143–147. doi: 10.1038/s41561-018-0288-0

Cleveland, W. S. (1979). Robust Locally Weighted Regression and Smoothing Scatterplots. *Journal of the American Statistical Association*, *74*(368), 829–836. doi: 10.2307/2286407

Cottrell, R. D., Tarduno, J. A., & Roberts, J. (2008). The Kiaman Reversed Polarity Superchron at Kiama: Toward a field strength estimate based on single silicate crystals. *Physics of the Earth and Planetary Interiors*, *169*(1-4), 49–58. doi: 10.1016/j.pepi.2008.07.041

Driscoll, P. E. (2016). Simulating 2 Ga of geodynamo history. *Geophysical Research Letters*, *43*(11), 2016GL068858. doi: 10.1002/2016GL068858

Glassmeier, K.-H., & Vogt, J. (2010). Magnetic Polarity Transitions and Biospheric Effects. *Space Science Reviews*, *155*(1), 387–410. doi: 10.1007/s11214-010-9659-6

Hawkins, L., Anwar, T., Shcherbakova, V., Biggin, A., Kravchinsky, V., Shatsillo, A., & Pavlov, V. (2019). An exceptionally weak Devonian geomagnetic field recorded by the Viluy Traps, Siberia. *Earth and Planetary Science Letters*, *506*, 134–145. doi: 10.1016/j.epsl.2018.10.035

Ingham, E., Heslop, D., Roberts, A. P., Hawkins, R., & Sambridge, M. (2014). Is there a link between geomagnetic reversal frequency and paleointensity? A Bayesian approach. *Journal of Geophysical Research: Solid Earth*, *119*(7), 5290–5304. doi: 10.1002/2014JB010947

Kissel, C., & Laj, C. (2004). Improvements in procedure and paleointensity selection criteria (PICRIT-03) for Thellier and Thellier determinations: Application to

Hawaiian basaltic long cores. *Physics of the Earth and Planetary Interiors*, *147*(2), 155–169. doi: 10.1016/j.pepi.2004.06.010

Kulakov, E., Sprain, C., Doubrovine, P., Smirnov, A., Paterson, G., Hawkins, L., … Biggin, A. (2019). Analysis of an updated paleointensity database (Q $_{PI}$ -PINT) for 65-200 Ma: Implications for the long-term history of dipole moment through the Mesozoic. *Journal of Geophysical Research: Solid Earth*, 2018JB017287. doi: 10.1029/2018JB017287

Lloyd, S. J., Biggin, A. J., Halls, H., & Hill, M. J. (2021). First palaeointensity data from the cryogenian and their potential implications for inner core nucleation age. *Geophysical Journal International*, *226*(1), 66–77. doi: 10.1093/gji/ggab090

Meert, J. G., Levashova, N. M., Bazhenov, M. L., & Landing, E. (2016). Rapid changes of magnetic Field polarity in the late Ediacaran: Linking the Cambrian evolutionary radiation and increased UV-B radiation. *Gondwana Research*, *34*, 149–157. doi: 10.1016/j.gr.2016.01.001

Merrill, R. T., McElhinny, M. W., & McFadden, P. L. (1996). *The Magnetic Field of the Earth: Paleomagnetism, the Core, and the Deep Mantle* (Vol. 63). Academic Press.

Nimmo, F. (2015). 9.08 - Thermal and Compositional Evolution of the Core. In G. Schubert (Ed.), *Treatise on Geophysics (Second Edition)* (pp. 201–219). Oxford: Elsevier.

Panovska, S., Constable, C. G., & Korte, M. (2018). Extending Global Continuous Geomagnetic Field Reconstructions on Timescales Beyond Human Civilization. *Geochemistry, Geophysics, Geosystems*, *19*(12), 4757–4772. doi: 10.1029/2018GC007966

Rodríguez-Mozos, J. M., & Moya, A. (2017). Statistical-likelihood Exo-Planetary Habitability Index (SEPHI). *Monthly Notices of the Royal Astronomical Society*, *471*(4), 4628–4636. doi: 10.1093/mnras/stx1910

Rosenqvist, L., Opgenoorth, H., Buchert, S., McCrea, I., Amm, O., & Lathuillere, C. (2005). Extreme solar-terrestrial events of October 2003: High-latitude and Cluster observations of the large geomagnetic disturbances on 30 October. *Journal of Geophysical Research: Space Physics*, *110*(A9). doi: 10.1029/2004JA010927

Selkin, P. A., & Tauxe, L. (2000). Long-term variations in palaeointensity. *Philosophical Transactions of the Royal Society of London. Series A: Mathematical, Physical and Engineering Sciences*, *358*(1768), 1065–1088. doi: 10.1098/rsta.2000.0574

Shue, J.-H., Chao, J. K., Fu, H. C., Russell, C. T., Song, P., Khurana, K. K., & Singer, H. J. (1997). A new functional form to study the solar wind control of the magnetopause size and shape. *Journal of Geophysical Research: Space Physics*, *102*(A5), 9497–9511. doi: 10.1029/97JA00196

Siscoe, G. L., & Chen, C.-K. (1975). The paleomagnetosphere. *Journal of Geophysical Research*, *80*(34), 4675–4680. doi: 10.1029/JA080i034p04675

Siscoe, G. L., & Sibeck, D. G. (1980). Effects of nondipole components on auroral zone configurations during weak dipole field epochs. *Journal of Geophysical Research: Solid Earth*, *85*(B7), 3549–3556. doi: 10.1029/JB085iB07p03549

Smirnov, A. V., Tarduno, J. A., Kulakov, E. V., McEnroe, S. A., & Bono, R. K. (2016). Palaeointensity, core thermal conductivity and the unknown age of the inner core. *Geophysical Journal International*, *205*(2), 1190–1195. doi: 10.1093/gji/ggw080

Tarduno, J. A., Blackman, E. G., & Mamajek, E. E. (2014). Detecting the oldest geodynamo and attendant shielding from the solar wind: Implications for habitability. *Physics of the Earth and Planetary Interiors*, *233*, 68–87. doi: 10.1016/j.pepi.2014.05.007

Tarduno, J. A., Cottrell, R. D., Bono, R. K., Oda, H., Davis, W. J., Fayek, M., ... Blackman, E. G. (2020). Paleomagnetism indicates that primary magnetite in zircon records a strong Hadean geodynamo. *Proceedings of the National Academy of Sciences*, *117*(5), 2309–2318. doi: 10.1073/pnas.1916553117

Tarduno, J. A., Cottrell, R. D., Davis, W. J., Nimmo, F., & Bono, R. K. (2015). A Hadean to Paleoarchean geodynamo recorded by single zircon crystals. *Science*, *349*(6247), 521–524. doi: 10.1126/science.aaa9114

Tarduno, J. A., Cottrell, R. D., Watkeys, M. K., Hofmann, A., Doubrovine, P. V., Mamajek, E. E., ... Usui, Y. (2010). Geodynamo, Solar Wind, and Magnetopause 3.4 to 3.45 Billion Years Ago. *Science*, *327*(5970), 1238–1240. doi: 10.1126/science.1183445

Tauxe, L., & Staudigel, H. (2004). Strength of the geomagnetic field in the Cretaceous Normal Superchron: New data from submarine basaltic glass of the Troodos Ophiolite: CRETACEOUS NORMAL SUPERCHRON. *Geochemistry, Geophysics, Geosystems*, *5*(2), n/a-n/a. doi: 10.1029/2003GC000635

Thallner, D., Biggin, A. J., & Halls, H. C. (2021). An extended period of extremely weak geomagnetic field suggested by palaeointensities from the Ediacaran Grenville dykes (SE Canada). *Earth and Planetary Science Letters*, *568*, 117025. doi: 10.1016/j.epsl.2021.117025

Thallner, D., Biggin, A. J., McCausland, P. J. A., & Fu, R. R. (2021). New Paleointensities From the Skinner Cove Formation, Newfoundland, Suggest a Changing State of the Geomagnetic Field at the Ediacaran-Cambrian Transition. *Journal of Geophysical Research: Solid Earth*, *126*(9). doi: 10.1029/2021JB022292

van der Boon, A., Biggin, A. J., Thallner, D., Hounslow, M. W., Bono, R., Nawrocki, J., ... Da Silva, A.-C. (2022). A persistent non-uniformitarian paleomagnetic field in the Devonian? *Earth-Science Reviews*, *231*, 104073. doi: 10.1016/j.earscirev.2022.104073

Voigt, G.-H. (1995). Magnetospheric Configuration. In *Handbook of Atmospheric Electrodynamics* (1st ed., Vol. 2, pp. 333–388). CRC Press. doi: 10.1201/9780203713297-11

Wood, B. E., Müller, H.-R., Zank, G. P., Linsky, J. L., & Redfield, S. (2005). New Mass-Loss Measurements from Astrospheric Lyα Absorption. *The Astrophysical Journal Letters*, *628*(2), L143. doi: 10.1086/432716

Ziegler, L. B., Constable, C. G., Johnson, C. L., & Tauxe, L. (2011). PADM2M: A penalized maximum likelihood model of the 0–2 Ma palaeomagnetic axial dipole moment. *Geophysical Journal International*, *184*(3), 1069–1089. doi: 10.1111/j.1365-246X.2010.04905.x